Applied Catalysis B: Environmental 300 (2022) 120742

Contents lists available at ScienceDirect

Applied Catalysis B: Environmental

journal homepage: www.elsevier.com/locate/apcatb

Mechanism investigation and product selectivity control on CO-assisted direct conversion of methane into C1 and C2 oxygenates catalyzed by zeolite-supported Rh

Takahiko Moteki [1,*], Naoto Tominaga [1], Masaru Ogura

Institute of Industrial Science, The University of Tokyo, 3-8-1 Komaba, Bunkyo-ku, Tokyo, Japan 153-8505

ARTICLE INFO

Keywords:
Zeolite
Methane
Methanol
Single-atom catalysis

ABSTRACT

Methane has emerged as an important energy source and chemical feedstock, and thus breakthrough strategies for the direct partial oxidation of CH_4 into small oxygenates have been desired. Here, CO-assisted CH_4 conversion towards C1 and C2 oxygenates over zeolite-supported single-atom Rh catalysts was demonstrated, and the key role of CO, as an indispensable additive, and the reaction mechanism were experimentally investigated. Step-by-step introduction of the reactants resulted in the formation of stoichiometric amounts of product. Replacement of O_2 by H_2O_2 revealed that gaseous O_2 acts as a true oxidant, and CO enhanced the reaction as a ligand. The critical effect of acid sites in the formation of the C_2 product was also confirmed. Based on these results, a plausible reaction mechanism was proposed. Finally, a small-pore zeolite, SSZ-13, was found to be superior for the selective production of methanol.

1. Introduction

Methane (CH_4) is the major component of natural gas (>70%) and has emerged as an important energy source and chemical feedstock since the shale gas revolution [1–3]. And, base-chemical production has shifted from the petrochemical to the natural gas industry. Methodologies for the direct partial oxidation of CH_4 into small oxygenates using gaseous O_2 as an oxidant have long been highly desired, and numerous studies have been dedicated to developing catalytic systems for such processes. Among them, the direct formation of methanol (CH_3OH) and its derivatives from CH_4 is a particularly active research area because of the enormous potential of CH_3OH as a fuel and base chemical. Accordingly, theoretical and experimental research extensively focused on catalyst design that can activate the C–H bonds without effecting over-oxidation to CO_2 over the years [4,5].

Many homogeneous and heterogeneous catalytic and chemical-loop systems (e.g., metal oxide catalysts [6–12], metal complex catalysts with strong acid [13–16], and metal-containing zeoltie [17–31] and MOF [32–36] materials) have been investigated for this purpose and summarized in different point of view [37–42], and numerous strategies for improving oxygenate yields have been employed, such as the use of reactive oxidants like N_2O [43–47] or H_2O_2. [48–51] Zeolite-supported transition-metal catalysts constitute a particularly interesting and promising class of catalytic materials for CH_4 oxidation [17–25]. In the last two decades, such catalysts have demonstrated good selectivities toward CH_3OH and other small oxygenates [37–42,52,53]. The structures of the active sites in Cu- and Fe-zeolites have been recognized similar to those of monooxygenase metalloenzymes [52–56], leading to a significant surge in their research. The sequential chemical-loop cycles protected methoxy species from overoxidation resulted in high CH_3OH selectivity. This process, however, makes such systems non-catalytic [27,28,57]. In some cases, it has been reported that some CH_4 oxidation was observed in catalytic route for such systems [30,31]. The oxygenate yields are, however, very low (typically less than 0.1%). Thus, exploring an effective catalyst and reaching a deeper understanding of such catalytic processes remain significant challenges in this field.

Another promising approach investigated by several groups is the use of carbon monoxide (CO) as an additive, which promotes C–H bond activation and lowers the reaction temperature required to form CH_3OH, formic acid (HCOOH), acetic acid (CH_3COOH) [58–70]. For instance, in the 1990s, Sen et al. demonstrated CO-assisted CH_4 conversion over the homogeneous [58] and heterogeneous [59–61] transition-metal catalysts, i.e., $RhCl_3$ and Pd/C, respectively. The latter provided HCOOH

* Corresponding author.
E-mail address: moteki@iis.u-tokyo.ac.jp (T. Moteki).
[1] Takahiko Moteki and Naoto Tominaga contributed equally to the paper.

https://doi.org/10.1016/j.apcatb.2021.120742
Received 23 May 2021; Received in revised form 17 September 2021; Accepted 19 September 2021
Available online 27 September 2021

formation from CH_4, CO, and O_2 in water at 358 K [59]. H_2O_2 formed from O_2 and H_2 was found as the actual oxidant for this system, which are derived from the water-gas shift reaction of CO with water [59]. In 2012, the formation of CH_3COOH over Zn-ZSM-5 from the reaction of CH_4, CO, and O_2 at 523–623 K was reported [62]. In that study, although the production of CH_3OH was not reported, the formation of surface methyl and methoxy species was confirmed. In 2015, Narsimhan et al. demonstrated the formation of CH_3OH and CH_3COOH over Cu-ZSM-5 and Cu-mordenite catalysts via chemical-loop processes, in which O_2, CH_4, and CO were added sequentially and the product was obtained by solvent extraction [63]. The reaction path to CH_3COOH was investigated in detail, and a Koch-type carbonylation mechanism was proposed [64–66], in which the methoxy molecules formed on Cu sites migrated to zeolite Brønsted acid sites and underwent subsequent CO insertion and hydrolysis of the acyl group to form CH_3COOH. Most recently, Rh-ZSM-5 was demonstrated as a potential catalyst for CO-assisted small-oxygenate production from CH_4 with high TON values of 200–2000, and CO was identified as a co-catalyst [67,68]. The role of CO is not yet fully understood, but it has been shown to be absolutely essential for oxygenates formation, and its coordination of Rh metal has been proposed in the previous studies [67,68].

Since these pioneering works, experimental and theoretical studies have addressed CO-assisted CH_4 oxidation over Rh-zeolite catalysts [69–71]. Specifically, density functional theory (DFT) studies have demonstrated that oxidative addition is the most plausible mechanism for CH_4 activation [71], rather than the commonly accepted metal-oxo mediated processes. In experimental studies, our recent work has revealed plausible routes for such reactions [69,70]. Unlike the industrialized CH_3OH-upgrading methods (i.e., the Monsanto and Cativa processes that manufacturing CH_3COOH from CH_3OH and CO), the Rh-ZSM-5 catalyst system does not result in the production of CH_3COOH from CH_3OH [69]. Therefore, the paths from CH_4 to C_1 oxygenates (CH_3OH and HCOOH) via partial oxidation and to the C_2 oxygenate (CH_3COOH) via oxidative carbonylation were investigated ~ as parallel reactions [69]. Nevertheless, Rh on Al_2O_3 and ZrO_2 supports was reported to catalyze CH_3OH carbonylation to CH_3COOH [72]. Thus, the details of the reaction mechanism and the role of CO remain to be revealed. Furthermore, new catalyst designs for higher product yield and selectivity remain to be established.

In the present study, the key factors for CO-assisted CH_4 conversion over zeolite-supported single-atom Rh catalysts were investigated experimentally, and Rh-SSZ-13 catalyst was found to demonstrate higher CH_3OH selectivity. The catalysts were prepared via a metal impregnation method. The relationship between the amount of metal loaded and catalytic activity showed a critical limit of around 0.5 wt%, where the major catalytic sites change from single atoms to clusters. Based on the catalytic tests, CO and O_2 were found to act as an indispensable additive and the true oxidant, respectively. Sequential addition of reactants suggested the formation of active oxygen-based species from CO and O_2 that subsequently react with CH_4. Furthermore, CH_4 was suggested to be activated in the presence of both CO and surface oxygen species, while it was not in the presence of CO alone. The use of H_2O_2, as a representative general oxidant that forms active oxygen species more easily than O_2, did not drastically enhance the formation of oxygenates, indicating that gaseous O_2 is a key reactant. The critical effect of acid sites in the formation of the C2 product (i.e., CH_3COOH) was confirmed by changing the Si/Al ratio of the zeolite and by ion-exchanging proton to alkaline metal cations. However, their role was found to be limited to the formation of CH_3COOH and not methane activation itself. With all the experimental results in hand, we proposed plausible reaction mechanisms for CH_3OH and CH_3COOH formation. Finally, the effect of zeolite framework structure was studied, and small-pore zeolites represented by SSZ-13 were found to be superior for the selective production of C1 oxygenates, most likely because the size of the pore window limits the formation of large products.

2. Experimental

2.1. Catalyst preparation

Four types of zeolites, sodium-form ZSM-5 (SiAl = 11.9), ammonium-form ZSM-5 (Si/A = 11.9), sodium-form mordenite (SiAl = 9), and sodium-form SSZ-13 (SiAl = 12), were supplied by Tosoh. Sodium-form ZSM-5 (SiAl = 45) was a JRC-Z5–90NA catalyst supplied by Japan Reference Catalysis. α-Al_2O_3 was purchased from Shimadzu Co. The sodium-form zeolites were preliminarily ion-exchanged to the NH_4-from before metal loading. As described in a previous report, [67–70] 4 g of sodium-form zeolite was dispersed in 200 mL of NH_4NO_3 (>99%, FUJIFILM Wako Pure Chemical) aqueous solution (1 M) and stirred at 353 K for 3 h, followed by drying in an oven at 373 K overnight. The procedure was repeated two times and ~3.6 g of the NH_4-form zeolites were finally obtained. Rh loading was conducted using the impregnation method [67–69]. Aqueous Rh solution (600 μL) was prepared from rhodium chloride ($RhCl_3{\cdot}nH_2O$, Rh 36–40%, Sigma-Aldrich) was added in 10 additions of 60 μL each to a 1 g of the NH_4-form zeolites. After impregnation, the obtained powder was treated in H_2 gas (5% balanced by Ar, Jyoto Gas) at 823 K for 3 h at a heating rate of 3 $K{\cdot}min^{-1}$ before catalytic tests.

2.2. Catalyst characterization

Thermogravimetric (TG) analyses were performed using a Thermo plus TG8120 (Rigaku) at a heating rate of 10 $K{\cdot}min^{-1}$ using the lab air feed as the carrier gas. Ammonia temperature programmed desorption (NH_3-TPD) measurements were conducted on a BELCAT (MICROTRAC MRB) equipped with a thermal conductivity detector. The sample was pretreated at 773 K for 60 min under He flow at a ramping rate of 10 $K{\cdot}min^{-1}$. Then, the sample was subjected to NH_3 gas (5% balance with He) at 373 K for 30 min before flushing with He for 15 min. NH_3-TPD spectra were recorded up to 883 K under He flow at a heating rate of 10 $K{\cdot}min^{-1}$. Metal dispersion measurements were performed using a BELCAT II (MICROTRAC MRB) by CO pulse adsorption method. The sample was pretreated at 723 K for 3 h under H_2 flow at a ramping rate of 5 $K{\cdot}min^{-1}$. Then, the sample was subjected to CO pulse at 323 K.

2.3. Catalytic evaluation

CO-assisted CH_4 conversion was conducted using a stainless-steel batch reactor. Briefly, 40 mg of catalyst, 8 mL of water, and a stirrer bar were placed in the reactor. The reactor was purged with N_2 gas, closed, and evacuated to around 6.7 kPa using a diaphragm pump. Then, 0.2 MPa of O_2, 0.5 MPa of CO, and 2.0 MPa of CH_4 were introduced sequentially. The reactor was placed in an oil bath at 423 K for a certain time, followed by water cooling for 15 min. The temperature inside the reactor placed in the oil bath is measured by K-type thermocouple and the profile has been shown in the previous publication. [69] As it requires between 40 and 60 min to reach to the set temperature, the reaction time was measured from the moment the reactor was placed in the oil bath. The gaseous reactants and products, CO, CH_4, and CO_2, were quantified by an on-line gas chromatography/methanation/flame ionization detection method using a Shimadzu GC-8A equipped with an active carbon column (length: 2 m, i.d.: 3 mm, particle size: 60/80 mesh). Methanation was conducted over a silica-alumina-supported Ni catalyst (80/125 mesh, Alfa-Aesar) at 623 K. The liquid phase was analyzed after removing the catalyst by centrifugation. Quantitative detection of CH_3OH, HCHO, HCOOH, CH_3CHO, and CH_3COOH was conducted using ^1H NMR with the DANTE pre-saturation pulse method at 303 K (JEOL JNM-ECS-400). Dimethyl sulfone was used as an internal standard.

2.4. Effect of experimental errors

To collect quantitative data for low-yield products and to ensure comparable and consecutive data between the different reactor batches, experimental errors were carefully considered. We found that several factors, including use of different gas loading port and different catalyst preparation lot for metal loading, were significant and needed to be considered. Tables S1–2 show the differences between three batches catalyzed with the same amount of catalyst prepared using the same preparation lot and reactant gas partial pressure, with using different gas-loading ports. The amounts of liquid-phase products are the average of three NMR measurements, indicating that the errors in the NMR data are caused by the low product yields. The results show that the standard deviation (1σ) can be up to 10% of the product amount, even though all the reactions and measurements were conducted under the same conditions. Therefore, we added 10% error bars to the product amounts.

3. Results and discussion

3.1. Effect of metal loading on product selectivity

In previous studies [67,68], the active sites of the supported Rh catalysts have been proposed to be single isolated Rh atoms. In general, the loading of monodisperse metal atom as an active catalytic site on a support material is a challenge, and a number of approaches to avoid formation of metal cluster have been applied for zeolite-supported catalysts [73–77]. In a previous study [67], the amount of Rh loaded onto ZSM-5 was varied from 0.1 to 1.0 wt% with showing a volcano-type activity plot, and the sample with Rh loading of 0.5 wt% was used as a model catalyst. Another study suggested that Rh nanoclusters form at a loading of 0.5 wt% [68]. These suggested that, as far as we follow the similar metal loading procedure, i.e., impregnation-type method, formation of Rh cluster was inevitable at metal amount of 0.5–1.0 wt%. Here, firstly, catalyst activity and product selectivity were measured along with metal loading of 0.002–5.0 wt% to observe the properties of metal site.

Fig. 1 shows the effect of metal loading on catalytic performance (production of CH_3OH, HCOOH, and CH_3COOH in liquid phase), where formation rates, C1/C2 selectivity, and Rh dispersion are shown as a function of metal loading. The measured Rh dispersion was in the range of 10–20% (Fig. 1 top), which would be lower than expected. It should be noted that the Rh amount is based on the preparation value due to the difficulty of accurate quantitative measurement of less than 0.1 wt% of Rh on the obtained samples. Therefore, qualitative comparisons between samples would be only sufficient to discuss. The change of Rh dispersion clearly changed over 0.5 wt% of Rh loading from about 17–10% (Fig. 1 top), which suggested that the aggregation of Rh occurred. If the loaded metal atoms acted as ideal catalytic sites, the reaction rate per metal amount would be constant and irrespective of metal loading, confirming the presence of monodisperse Rh sites without aggregation or clustering. The observed rate, however, slightly decreased with increasing Rh loading of 0.002–0.5 wt%, which indicates that not all the metal atoms act as uniform catalytic sites. Besides the formation of clusters or nanoparticles, the loading of metal atoms at inaccessible positions within the zeolite framework, i.e., formation of inert sites, would be another probability, as seen elsewhere. [78,79] Although the observed product formation rates decreased along with the Rh loading in that range, the C1/C2 ratio of the products were constant in this range (Fig. 1 middle). This indicates that the formed accessible catalytic sites possessed similar properties. However, above 0.5 wt%, formation rates of methanol and formic acid showed more severe decrease than their lower metal loading range although that of acetic acid did not (Fig. 1 bottom). Thus, the C1/C2 ratio drastically decreased, indicating the higher product selectivity towards C2 product, i.e., CH_3COOH (Fig. 1 middle). This strongly suggests the rapid decrease of the amount of predominant single atom Rh site by aggregation and

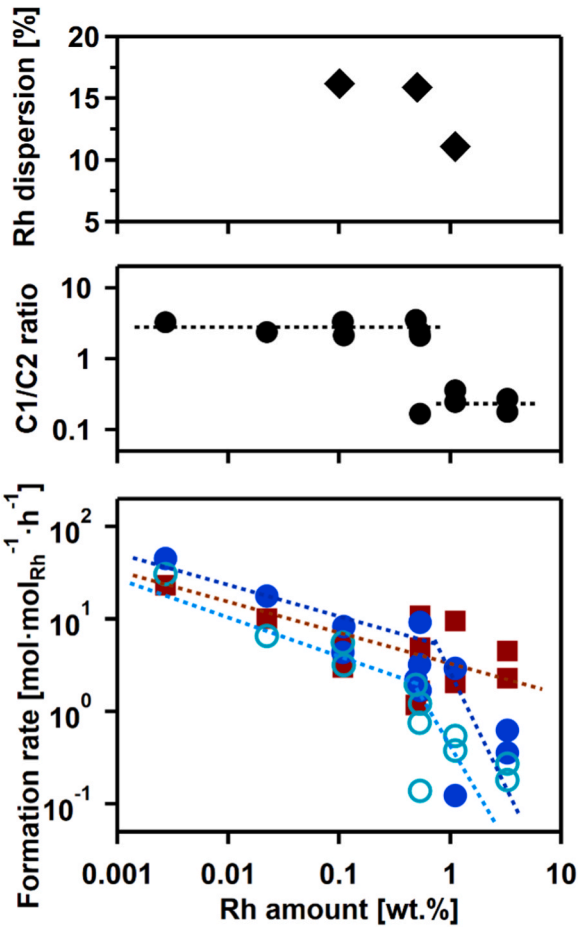

Fig. 1. Formation rate of liquid products as a function of Rh loading for ZSM-5 zeolite (bottom) and C1/C2 ratios (middle) (0.2 MPa O_2, 0.5 MPa CO, 2.0 MPa CH_4, 40 mg catalyst, 8 mL water, 423 K), and Rh dispersions measured by CO pulse adsorption (top). In the bottom graph, light-blue open circles, blue filled circles, and red filled squares represent methanol, formic acid, and acetic acid, respectively. Dashed lines are added as a guide.

formation of another site, which would be favorable for the formation of C2 product. Because it only observed at higher metal loading range with the decrease of Rh dispersion, the estimated new site would be metal clusters or nanoparticles. In previous studies [67,68], only below 0.5 wt % of metal loadings, the formation of monodisperse Rh sites was confirmed directly and indirectly by techniques including HAADF-STEM, EXAFS, XPS, and probe-IR, showing good agreement with our observations. Therefore, it can be assumed that an atomically dispersed Rh catalyst was also successfully prepared in this study within the Rh loading of 0.002–0.5 wt%. Accordingly, in the following sections, catalysts with an Rh loading of 0.1 wt% were mainly used for the catalytic tests to assume a contribution of monodisperse Rh site as a catalytic site. To achieve a higher loading of active Rh site, other preparation methods (e.g., ion-exchange and direct synthesis [70]) or other supports should be tested in the future. Furthermore, higher selectivity towards acetic acid over high Rh loading catalyst would be another potential target [69].

3.2. Stepwise introduction of reactants to investigate the key species

The state of catalytic site, the key step of CH_4 activation (most plausibly C–H activation), and the corresponding role of CO are still under discussion. For the widely discussed Cu- and Fe-zeolite catalysts, the formation of active metal-oxo species is considered critical for CH_4 activation [20–31]. For Rh-zeolite catalysts, molecular oxygen

coordinated Rh was initially proposed as an active site based on experimental studies and computational DFT analyses [67,68]. At the same time, the DFT study suggested Rh-oxo species was also a potential candidate to activate CH_4. However, a recent DFT study indicated that oxidative addition of CH_4 to a ligand (H_2O) coordinated Rh is the critical C–H bond cleavage step [71]. Here, we derived a plausible reaction mechanism via an experimental approach, in which the stepwise introduction of reactants was conducted to investigate the critical reaction step and surface species.

Table 1 compares the amounts of product formed via two different sequences of reactant introduction. In case 1, CO and O_2 were added first and the reactor was heated at the reaction temperature of 423 K for 2 h, where the formation of surface oxygen-based species was expected. After the reactor was cooled, the gases were removed with a flange pump and the reactor was filled with CH_4 and heated again to the reaction temperature for 2 h. In case 2, CH_4 and CO were added first and then O_2. The amount of obtained products (Table 1) clearly showed that only case 1 provides measurable amounts of products. Furthermore, the product to Rh site ratio was almost one (1.05), showing the stepwise reaction proceeded in a stoichiometric manner. The results also indirectly suggested that the most of loaded Rh metal successfully worked as a monodispersed active site. In this experiment, we expected that the surface species formed during step 1 (such as oxo, oxygen, methyl, or methoxy) would remain during the degassing process and present in step 2, otherwise the experimental results would not be explained. The coordination of CO is generally strong on Rh metal, and thus cases 1 and 2 compare the formation of active surface species formed via O_2 and CH_4, respectively. For case 1, we assumed that the key active species for CH_4 activation are surface oxo species formed with the help of CO ($CO + O_2$ + Rh-zeolite → CO_2 + O═Rh-zeolite). Case 2 supposed that CH_4 was activated over ligand-coordinated (i.e., either CO or H_2O) Rh, as per the previous study [71]. Because our tests did not mimic the sequence of the elementary reaction steps proposed in the previous studies [67,68,71], the results neither support nor disprove any particular case for the previous works. The key observation provided here would be 1) the formation of active oxo or coordinated oxygen species at Rh sites and 2) the reaction of CH_4 with those surface species in the subsequent step (Case 1). These discussions and results would support the early studies proposing an oxygen-based species as a key to activate CH_4 [67,68], rather than the DFT study suggesting an oxidative addition as a critical step [71]. In the early works [67,68], initially adsorbed O_2 molecule was described as a critical species for reductive elimination of H from CH_4. On the other hand, we supposed that surface oxo-like species would be a key species for CH_4 activation, which can be more feasible to explain the quite fast CO oxidation (side reaction) [69] and the lower energy barrier of the route calculated in the other DFT study [71]. Details are discussed in the following section about reaction mechanism investigation.

3.3. Gaseous oxygen as an oxidant

The choice of oxidant is the most critical factor in oxidation reactions. Besides gaseous O_2, H_2O_2 [48–51], and N_2O [43–47] have also been reported as potential oxidants over Fe- and Cu-zeolites. In our system, H_2O was used as the solvent, so H_2O_2 might be formed via the water-gas shift (WGS) reaction of CO. Furthermore, H_2O_2 is generally known as an effective oxidant to produce surface oxo-species. Thus, CO and O_2 added in the system might be replaced by solo H_2O_2. To identify the true oxidant in the reaction and to demonstrate the replacement for CO and O_2, control reactions with H_2O_2 were performed.

Fig. 2 summarizes the results of catalytic tests conducted with and without potential oxidants. In the presence of CO and H_2O_2 instead of gaseous O_2, the successful formation of oxygenates was observed and their amounts were comparable with those for gaseous O_2. Under the test conditions, i.e., 0.3 mL of 30 wt% aqueous H_2O_2 solution, the amount of O_2 gas formed from the simple decomposition of all the H_2O_2 molecule ($2H_2O_2 \rightarrow 2H_2O + O_2$) is around 3×10^3 μmol per reactor, which is almost the same as that for the conventional reaction conditions (an O_2 amount of 2.3×10^3 μmol per reactor). It should be noted that CO was also a critical additive in the case of H_2O_2. Even though the formation of small amount of CH_3OH in the absence of CO (Fig. 2) suggested the successful formation of active oxygen species from solo H_2O_2, it was not as effective as generally assumed. It is recognized that H_2O_2 is a stronger oxidant because it easily forms active oxygen (or oxo) species ($H_2O_2 \rightarrow O + H_2O$), and in many cases, use of H_2O_2 instead of gaseous O_2 results in superior oxygenate formation and catalytic activity. Furthermore, if H_2O_2 forms via WGS reaction as a true oxidant in the reaction, direct use of H_2O_2 would result in superior oxygenate formation compared to the reference reaction with O_2 and CO. Therefore, it is suggested that H_2O_2 decomposed during the reaction and generated gaseous O_2 worked as the actual oxidant. In fact, the generation of bubbles from the H_2O_2 solution was observed just after adding the zeolite catalyst, even under the room temperature and ambient pressure conditions. These data clearly indicate that the true oxidant is gaseous O_2 while H_2O_2 itself does not work as an effective oxidant.

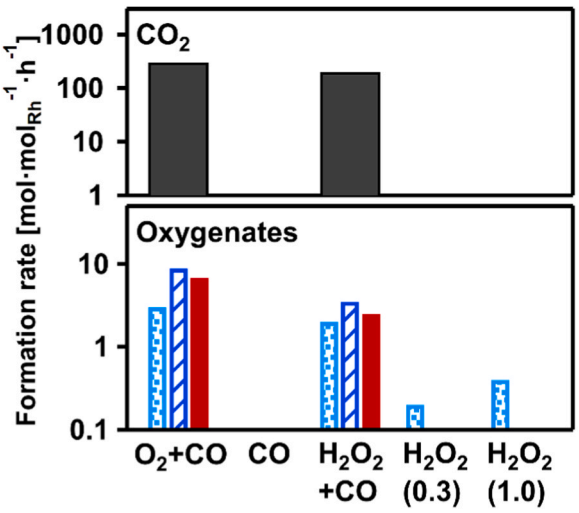

Fig. 2. Product oxygenate (bottom) and CO_2 (top) formation rates over Rh-ZSM-5 using gaseous O_2 or H_2O_2 as an oxidant with or without CO. In the bar graph (bottom), the left bar with light-blue dots, the middle bar with blue stripes, and the right bar with filled red indicate methanol, formic acid, and acetic acid, respectively.

Table 1
Gas introduction sequence and the results of the catalytic reaction.

Case #	Reaction condition[a]		Catal amount [mg]	CH_3OH [μmol]	HCOOH [μmol]	CH_3COOH [μmol]	Product/Rh [mol/mol]
	Step 1	Step 2					
Case 1	O_2 + CO	CH_4	43.2	0.48	-[b]	1.71	1.05
Case 2	CH_4 + CO	O_2	42.5	–	–	–	–

[a] The detailed reaction procedures are given in supporting information. Basically, the partial pressure of reactant gas and the amount of catalyst and solvent water were sane as the conventional reaction condition (0.2 MPa O2, 0.5 MPa CO, 2.0 MPa CH4, 40 mg catalyst with Rh loading of 0.5 wt%, 8 mL water, 423 K).
[b] The amount was lower than the detection limit.

Furthermore, together with the conclusions about the role of CO drawn in the above section, the current results provide further insight into the reaction mechanism. Because measurable amount of CH_3OH formed in the case with solo H_2O_2 (Fig. 2), a successful formation of oxygen species can be proposed. Thus, its lower reactivity might suggest that CO is also critical for the subsequent CH_4 activation step as a ligand besides for the formation of surface oxo-species as a reductant. Here, coordinated CO could be maintained between steps 1 and 2 (Table 1) and play some role in the latter step. Although these conclusions, proposing key reaction steps, would require further studies to ensure the critical role of CO, the above results certainly indicate the key role of CO as a reductant to form surface oxo species and as a ligand to coordinate Rh to form active catalytic sites.

3.4. Role of acid sites for CH_3COOH production

Although the metal sites play a major role in the catalytic reaction, acid sites could also contribute to the reaction. Previous work by Román et al. suggested that zeolite acid sites are critical for CH_3COOH production over Cu-mordenite catalysts [63]. Their study revealed that methyl species formed on unique Cu sites migrate to Brønsted acid sites forming localized methoxy groups, which underwent the subsequent CO addition (carbonylation) towards CH_3COOH [63]. For Rh-zeolite catalysts, the zeolite Si/Al ratio of 15 has shown to be better than that of 100, although the reason for this was not fully investigated [67]. And drastic decrease in the production of CH_3COOH over Na ion-exchanged ZSM-5 was also reported [67]. Accordingly, in the present study, the role of acid sites was further investigated to better understand the full reaction characteristics.

Fig. 3 shows the amounts of total oxygenates and their C1/C2 ratios formed over Rh-loaded MFI-type zeolites with different Si/Al ratios. It should be noted that, in this study, metal loading was conducted with NH_4-form zeolites, and the subsequent thermal treatment results in the formation of metal-loaded H-form zeolites. Except for pure silica case (i.e., a Si/Al ratio of infinity, known as silicalite-1), the changes in total oxygenate formation along with reaction time were similar (Fig. 3, bottom). However, differences in the C1/C2 ratios of the products were observed (Fig. 3, top). The catalysts with lower Si/Al ratios (12 and 20) provided products with lower C1/C2 ratios, indicating the formation of more CH_3COOH (Fig. 3). Thus, catalysts possessing more acidic sites (or Al sites) favor the formation of C2 products from C1 reactants. If we assume that the kinetically relevant step is the initial C–H bond activation of CH_4 catalyzed by the metal site, the observed total oxygenates formation may be explained based on the similar metal loadings of the catalysts, which are independent of acid-site abundance. Thus, the observed product selectivities (Fig. 3, top) may be explained by the contribution of acid site in the subsequent step toward C2 product. These assumptions agree with the data in Fig. 1 well, where the metal loading of zeolites was varied with a constant Si/Al ratio of 12. The C1/C2 selectivities do not change as long as the metal atoms remain as a single-atom sites (Fig. 1, top). These results indicate the catalytic Rh sites prepared over zeolites with different Si/Al ratios possessed similar properties for CH_4 activation. In other words, CH_4 activation step are assumed to be unaffected by the acidity (i.e., Si/Al ratio) of the zeolite support as far as Rh works as a single-atom catalytic site. In the case of pure silica zeolite support, total oxygenates formation was less than half compared to aluminosilicate ones. We assume that this is due to the formation of Rh clusters (or nanoparticles) despite the same metal loading amount. In general, zeolite acid sites also work an ion-exchange sites, which would have some positive effects on the monodisperse distribution of the metal (although Rh was loaded via an impregnation method in this study).

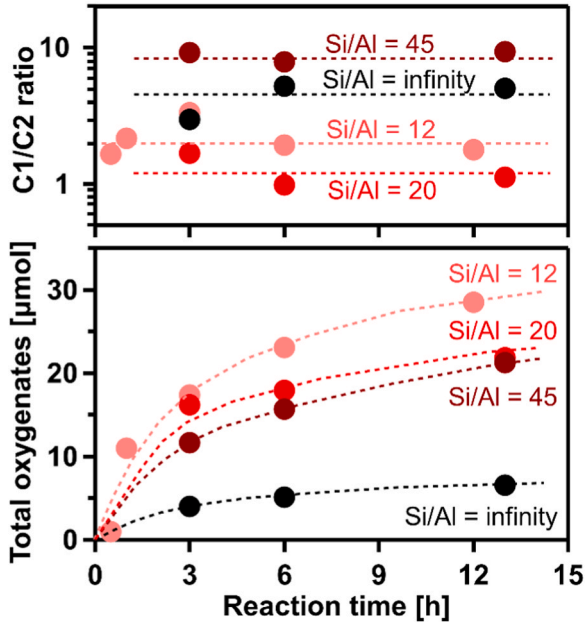

Fig. 3. Changes of total oxygenate amounts with reaction time over Rh-ZSM-5 with different Si/Al ratios of 12 (light-red circles), 20 (red circles), 45 (brown circles), and pure silica (black circles), and the C1/C2 ratios (top) (0.2 MPa O_2, 0.5 MPa CO, 2.0 MPa CH_4, 40 mg catalyst, 8 mL water, 423 K).

The contribution of acid sites towards product selectivity was also confirmed using ion-exchanged catalysts. Further ion-exchange of proton to alkaline metal cations (Li^+, Na^+, K^+, Cs^+) was conducted after metal impregnation. The loss of Brønsted acid sites due to this ion-exchange was confirmed by NH_3-TPD measurements (Fig. S5 in Supporting Information). Fig. S6 shows the product formation rates per metal site and their C1/C2 ratios for the parent Rh-ZSM-5 catalyst and the ion-exchanged catalysts. The Brønsted acid sites clearly play a critical role in C2 product formation, and ion-exchanging these sites with alkali metal hinders C2 production, which showed a similar trend as demonstrated before [67]. The production of C2 oxygenates was not completely suppressed to zero, which suggests the presence of another C2 production route without acid sites. It should be noted that the total oxygenates formation was decreased after ion-exchange (Fig. S6), i.e., the lost C2 amount was not fully compensated by the increase of C1 production to keep the steady CH_4 activation rate as mentioned above. This would be because of some effect of metal cation towards Rh site and/or towards reaction site. These results (Fig. 3 and S6) support the conclusion that the catalytic sites for CH_4 activation (most plausibly, initial C–H bond cleavage) and subsequent C1 oxygenates production are single-atom Rh sites. C2 production over the metal site is possible but it is a minor route. Acid site would mostly contribute on the subsequent CO insertion step after CH_4 activation towards C2 production as a major product, which itself would not catalyze CH_4 activation.

3.5. Reaction step of CO-assisted direct CH_4 conversion over Rh-ZSM-5

A plausible important reaction step based on the above results and discussion may be proposed here. As CO is a critical additive, its role is key in the reaction. The previous *ex-situ* spectroscopic study revealed the coordination of CO to Rh^I [67,69], which was a reduced state from the Rh source ($RhCl_3$) and suggested the role of CO as a ligand to promote the catalysis by Rh. However, another plausible possibility is that it acts as a reductant to generate active O species. Here, in this study, some new clues were obtained, i.e., 1) stepwise introduction of reactant gases in a specific order (Table 1) generates the oxygenate products, indicating the formation of active O species from O_2 and CO; 2) gaseous O_2 is critical for the reaction (Fig. 2) and, in the absence of O_2, CO and CH_4 do not form CH_3OH, acetaldehyde (CH_3CHO), or CH_3COOH; and 3) presence of Brønsted acid site promotes C2 oxygenate (CH_3COOH) formation (Fig. 3) while Rh site itself also can form CH_3COOH without acid sites

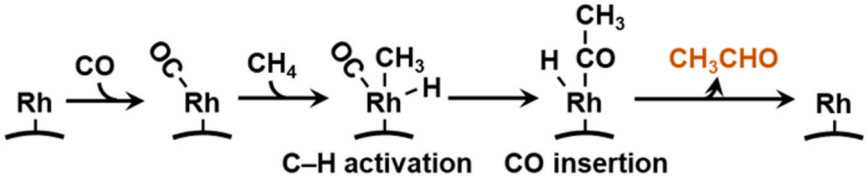

Scheme 1. Speculated mechanism of C–H activation over CO-coordinated Rh.

(Fig. S6). Although these observations are not sufficient to provide a complete picture, a plausible role of CO and a reaction mechanism may be drawn, as presented below.

If CO only works as a ligand of Rh, and the coordinated Rh can perform CH_4 activation (i.e., C–H bond cleavage) via a nucleophilic metal insertion reaction [42], it might form CH_3CHO without the presence of O_2, as shown in Scheme 1. Both the CO insertion step and the subsequent formation of CH_3CHO (Scheme 1) could proceed under presence of H_2O based on both the above discussion point 3 and the previous reports [80–82]. Our results (Table 1 and the above points 1 and 2), however, do not support this hypothesis. This suggests that the key species for CH_4 activation is neither the solo Rh sites nor CO-coordinated Rh sites alone. Another potential species contributing to CH_4 activation would be adsorbed O_2 or O species. Contribution of adsorbed O_2 onto Rh was initially proposed in the literatures [67,68]. Here, however, we designed our experiments (Table 1) to assume that the surface O (or oxo) rather than O_2 would be the key species. Surface O species may form on Rh via oxidation of coordinated CO ($CO^* + O_2 \rightarrow CO_2 + O^*$) and/or, less plausibly, via rapture of adsorbed O_2 ($O_2^* + * \rightarrow 2O^*$), which might insert into C–H bonds ($M{=}O + CH_4 \rightarrow CH_3{-}M{-}OH$) as shown in Scheme 2 (C–H activation). Although the step is described in the scheme as a sigma-bond-metathesis-like reaction, simple H-abstraction by active O species and subsequent methyl radical adsorption on the metal could be another potential cause of CH_4 activation. [42] We assume that both O_2 and CO allow the formation of active O species, and the experimental results (Table 1 and point 1) are consistent with this assumption. Furthermore, the direct formation of CH_3COOH as a C2 oxygenate (path 3 in Scheme 2) might explain the observation of neither direct carbonylation of CH_3OH to CH_3COOH nor CH_3CHO intermediate in the previous study, [69] which was previously explained by its high reactivity toward CH_3COOH [69]. Moreover, based on the data in Fig. 2, only the presence of active O species (that was achieved using H_2O_2 without CO) does not strongly catalyze the reaction. This indicate that coordinated CO as well as active O is also necessary for high catalytic performance, and thus paths 2 and 3 are more feasible than path 1 in Scheme 2. It should be noted that the formation of active O would be accompanied by equimolar CO_2 formation, which would not explain the formation of the huge amount of CO_2 observed in the previous study [69]. As a side reaction, the formation of CO_2 from the active O reacting with CO (Path 4 in Scheme 2) is reasonable. This path seems to be much easier than the competing target routes, i.e., CH_4 activation (paths 2 and 3 in Scheme 2), and this speculation agrees well with previous results [67,68]. Again, both O_2 and O species shown in the previous [67,68] and present studies were plausible species for CH_4 activation proposed via experimental approaches. Although these two cases would simultaneously proceed over the catalysts and does not conflict each other, we suggest the O (or oxo) species formed from CO and O_2 would be more plausible case. This is based on 1) the observation of much faster CO oxidation by O_2 (as a side reaction) in our previous work [69] suggesting the higher reactivity of these two reactants, and 2) the lower energy barrier on the metal-oxo route rather than adsorbed O_2 route based on the previous DFT study [71]. A clearer picture will be provided by further studies.

3.6. Catalyst design for the selective production of methanol

Currently, industrial production of CH_3OH from CH_4 is performed by syngas-based routes. On the other hand, the direct conversion of CH_4 (i.e., partial oxidation) using abundant gaseous O_2 as an oxidant is an extremely desirable alternative. The CH_3OH yields of reactions are well discussed indicators and are frequently compared in this field. The conversion of CH_4 and selectivity toward CH_3OH generally exist in a trade-off relationship [37,42], and many attempts have been made to achieve high CH_3OH yields. Among the catalysts reported thus far, metal-loaded zeolite catalysts demonstrate high selectivity (>80%) but low CH_4 conversion (<1%) [37].

As is shown by the present study, CO-assisted CH_4 conversion over Rh-ZSM-5 forms useful oxygenates besides CH_3OH, i.e., HCOOH and CH_3COOH [67–69]. Among them, CH_3COOH may be a potential target product because it behaves as a terminal product due to its slow over-oxidation [69]. Here, however, we have concentrated on a "dream reaction," i.e., selective CH_3OH production. In previous studies, it has been shown that CH_3OH can be overoxidized to HCOOH and finally CO_2 [69], and that CH_3OH selectivity over Rh-ZSM-5 catalysts is not high. New catalysts and/or reaction condition optimization should be necessary to increase CH_3OH selectivity. We have demonstrated that some platinum-group metals (i.e., Ru, Ir, and Pd) besides Rh could be potential catalysts showing different product selectivities [69].

Another approach to controlling product selectivity would be exploiting the size (or shape) selectivity of the zeolite support. Because the kinetic diameter of CH_3OH is the smallest among the obtained oxygenates, size-selective production would be possible with the proper choice of zeolite framework. ZSM-5 zeolite possesses an MFI-type framework structure, in which straight 10-membered-ring (MR) channels and 10-MR zigzag channels form a three-dimensional medium pore structure. The pore-opening size and internal void space of ZSM-5 zeolite are larger than the kinetic diameter of all the obtained products, meaning that the steric interaction between the products and the zeolite framework would not be strong enough to impart size/shape selectivity. Thus, small-pore zeolites, generally those with 8 MRs as the largest pore opening (such as CHA-, AFX-, and AEI-type frameworks) may restrict large-product formation [83].

Fig. 4 shows the product-formation rates over Rh supported on different zeolite framework structures and

α-Al_2O_3, and their C1/C2 product ratios. As well as the MFI-type structure, MOR-, CHA-, and AFX-type zeolites with Si/Al ratios of 9, 12, and 4.6, respectively, were evaluated. MOR-type zeolite is classified as large-pore zeolite due to its 12-MR straight channels crossing with 8-MR channels. CHA- and AFX-type zeolites are small-pore zeolites possessing 8-MR pore openings and cage-like internal voids. The pore openings of CHA- and AFX-type frameworks are ~3.7 Å [84], which is much smaller than the kinetic diameter of the obtained C2 oxygenate, CH_3COOH (4.36 Å) [85,86]. The C1/C2 ratios (Fig. 4) clearly show that small-pore zeolites (CHA and AFX) are more selective for C1 oxygenate production. These results indicate that most of the reaction proceeds inside the zeolite pore as well as confirming the successful loading of the metal atoms into the pores, which is sometimes a challenge with

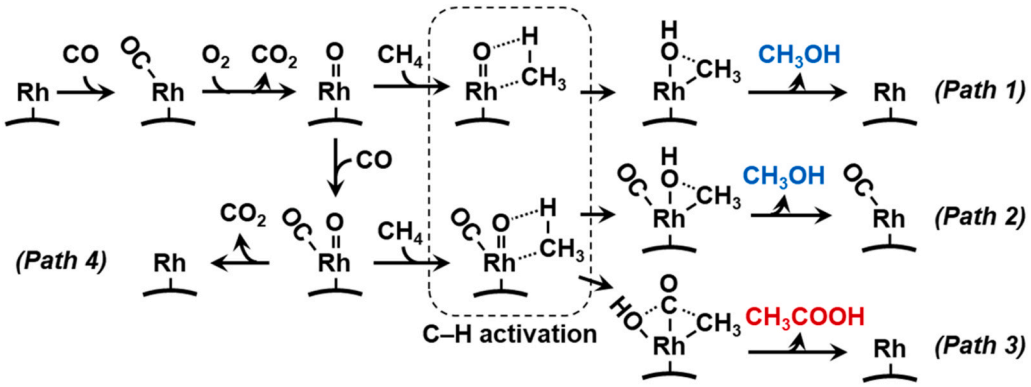

Scheme 2. C–H activation with the help of surface O species over bare or CO-coordinated Rh, and subsequent oxygenate formation.

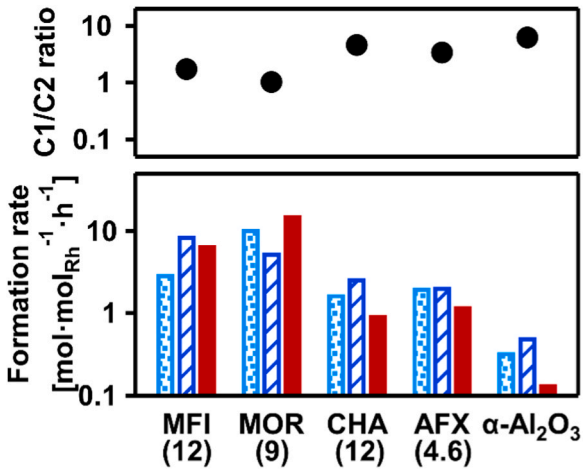

Fig. 4. Formation of oxygenates and their C1/C2 ratios over Rh supported by an MFI-type structure (i.e., reference ZSM-5) and by MOR-, CHA-, and AFX-type structures and α-Al_2O_3 (0.2 MPa O_2, 0.5 MPa CO, 2.0 MPa CH_4, 40 mg catalyst, 8 mL water, 423 K, 6 h). In the bar graph (bottom), the left bar with light-blue dots, the middle bar with blue stripes, and the right bar with filled red indicate methanol, formic acid, and acetic acid, respectively.

small-pore zeolites. Interestingly, in the case of the AFX-type zeolite, even though the framework has the low Si/Al ratio of 4.6 (i.e., possessing more acid sites), the C1/C2 ratio is much higher than that for the MFI-type zeolite, which has a Si/Al ratio of 12. These results indicates that the zeolite framework structure has a larger effect upon product selectivity. However, still it is not clear that whether the pore size is the direct reason for these structure-depending product selectivity. The state of Rh, i.e., the formation of small clusters or nanoparticles besides single-atom site, would also be affected by the framework types. Recently, unique structure-depending product selectivities have shown over cage-type Rh-zeolites, [83] while their relationships were not explained by a single physicochemical property. More precise and controlled comparative experiments should be required to figure out the critical factor for product selectivities. In the case of α-Al_2O_3, the side reaction (i.e., CO oxidation to CO_2) proceeds more than that over the zeolites, and the overall reaction is suppressed, maybe due to the formation of Rh nanoparticles. This is a similar trend to that observed in the case of silicalite-1 (Fig. 5). Among the tested catalysts, CHA-type zeolite with Si/Al ratio of 12 was further investigated.

Fig. 5 shows the product profiles and C1/C2 selectivities along with the reaction time for Rh-ZSM-5 (left) and Rh-SSZ-13 (right) catalysts (y-axis is shown in log scale). Over Rh-ZSM-5 catalyst (Fig. 5 left), as also previously shown, [69] the amounts of CH_3OH and HCOOH decreased after reaction time of 30 h. This has been explained by the combination

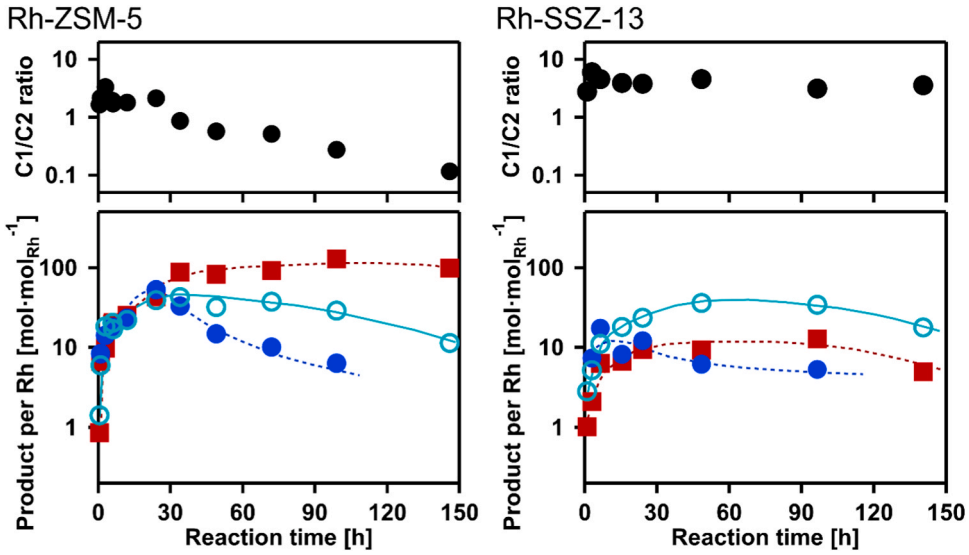

Fig. 5. Changes of the amount of oxygenates formed along with reaction time over Rh-ZSM-5 and Rh-SSZ-13 catalysts, and the C1/C2 ratios (top) (0.2 MPa O_2, 0.5 MPa CO, 2.0 MPa CH_4, 40 mg catalyst, 8 mL water, 423 K). In the bottom graph, light-blue open circles, blue filled circles, and red filled squares represent methanol, formic acid, and acetic acid, respectively.

of 1) overoxidation of products into CO_2 and 2) stop of the reaction due to the unintended consumption of CO by side reactions. [69] CH_3COOH reached a steady amount at around 30 h because of its much slower overoxidation [69]. This results in a decrease in C1 selectivity with time (Fig. 5 left). Conversely, the Rh-SSZ-13 catalyst showed high CH_3OH selectivity throughout the reaction (Fig. 5 right). The CH_3OH formation rates per Rh metal are almost the same for these two frameworks, which suggests the presence of similar catalytic sites and that the formation of CH_3OH is not hindered by the small-pore structure of SSZ-13. However, CH_3COOH formation (red squares in Fig. 5) is suppressed by more than one order of magnitude over Rh-SSZ-13. HCOOH formation is also suppressed, especially in the early stage of the reaction (up to 30 h). The drastic decrease in CH_3COOH formation results in a high C1/C2 ratio and high CH_3OH selectivity for Rh-SSZ-13 (Fig. 5 right top). Because both zeolites have similar a Si/Al ratio (12), their difference in selectivity may be explained by 1) different catalytic sites and/or reaction space unfavorable to CH_3COOH formation; and/or 2) limited diffusivity of the small 8-MR pore opening. However, because the total amount of oxygenates was not maintained by changing the zeolite framework from MFI to CHA, it is difficult to judge the critical reason for the product selectivity at this moment. For the formation of CH_3COOH, the contribution of acid sites (Al sites) is expected, as discussed above. Theoretically, for an Si/Al ratio of 12, one Al site exists per CHA cage. One explanation would be the difficulty in forming catalytic sites that allow simultaneous access of both CH_4 and CO to Rh and acid sites owing to the steric effect of the cage structure. And that resulted in the catalytic site being more selective toward C1 products but less reactive for CH4 conversion. Another possibility would be the limited diffusion of the formed CH_3COOH through the 8-MR window, while catalytic activity of Rh site itself was maintained over different zeolite frameworks. In this case, accumulation of large organic products inside the cage would be a direct cause of the catalyst deactivation. However, no weight loss due to the combustion of any remaining organics was observed by TG analysis, and no color change of the catalyst was observed after the catalytic tests (data not shown). These facts suggest that the formed C2 products were simultaneously and promptly overoxidized to CO_2 inside the cages. Again, above both explanations are plausible at this moment, and further studies should be necessary to explain the critical reason of the product selectivity derived from zeolite frameworks. As shown in this section, the zeolite framework is a critical factor in oxygenate production. This finding may prompt other zeolite framework structures to be considered. In future research into metal-loaded zeolite catalysts for CO-assisted direct CH_4 conversion, it may be necessary to focus on the "site property" formed in unique zeolite frameworks rather than their pore (and window) size.

4. Conclusions

CH_4 conversion into small oxygenates was conducted at low temperature of 423 K over zeolite-supported Rh catalysts with the help of CO using gaseous O_2 as an oxidant. Critical factors of the reaction and roles of CO were experimentally investigated in the first part of this manuscript. The changes in the product formation rates and selectivity along with the amounts of Rh metal loading suggested that, for a metal loading of 0.5 wt% or more, Rh nano particle or cluster would be formed besides single-atom Rh sites. And C2 oxygenate, CH_3COOH, was more selectively formed over those particle or cluster containing Rh-ZSM-5. Step-by-step introduction of the reactants, the use of H_2O_2 as an alternative oxidant, and acid-site control by the change of Si/Al ratio or by the ion-exchange with alkaline metal cation, allowed us to suppose the critical roles of CO as a reductant, a ligand, and a reactant. Based on these results, a plausible reaction step was proposed. CH_4 is activated by surface oxygen-based species (e.g., surface oxo-species) formed by the reaction of CO and O_2. The subsequent release of methoxy or CO insertion provides CH_3OH or CH_3COOH, respectively, as primary products. And, in the second part, the selective production of C1 oxygenates (CH_3OH and HCOOH) was achieved using a small-pore zeolite as a Rh support, demonstrated in this study with SSZ-13 as a representative zeolite. This catalyst provided the C1 oxygenate as the major product by suppressing the formation of CH_3COOH.

CRediT authorship contribution statement

Takahiko Moteki: Conceptualization, Methodology, Writing - reviewing and editing. **Naoto Tominaga**: Data curation, Writing - original draft preparation. Visualization, Investigation. **Masaru Ogura**: Reviewing and editing, Supervision.

Declaration of Competing Interest

The authors declare that they have no known competing financial interests or personal relationships that could have appeared to influence the work reported in this paper.

Acknowledgements

The authors would like to acknowledge Nippon Sheet Glass Foundation for Materials Science and Engineering for funding.

Appendix A. Supporting information

Supplementary data associated with this article can be found in the online version at doi:10.1016/j.apcatb.2021.120742.

References

[1] R.H. Crabtree, Aspects of methane chemistry, Chem. Rev. 95 (1995) 987–1007, https:/doi.org/10.1021/cr00036a005.
[2] N.J. Gunsalus, A. Koppaka, S.H. Park, S.M. Bischof, B.G. Hashiguchi, R.A. Periana, Homogeneous functionalization of methane, Chem. Rev. 117 (2017) 8521–8573, https://doi.org/10.1021/acs.chemrev.6b00739.
[3] R. Horn, R. Schlogl, Methane activation by heterogeneous catalysis, Catal. Lett. 145 (2015) 23–39, https://doi.org/10.1007/s10562-014-1417-z.
[4] A.A. Latimer, A. Kakekhani, A.R. Kulkarni, J.K. Nørskov, Direct methane to methanol: the selectivity-conversion limit and design strategies, ACS Catal. 8 (2018) 6894–6907, https://doi.org/10.1021/acscatal.8b00220.
[5] S.J. Blanksby, G.B. Ellison, Bond dissociation energies of organic molecules, Acc. Chem. Res. 36 (2003) 255–263, https://doi.org/10.1021/ar020230d.
[6] R. Pitchai, K. Klier, Partial oxidation of methane, Catal. Rev. Sci. Eng. 28 (1986) 13–88, https://doi.org/10.1080/03602458608068085.
[7] N.R. Foster, Direct catalytic oxidation of methane to methanol – a review, Appl. Catal. 19 (1985) 1–11, https://doi.org/10.1016/S0166-9834(00)82665-2.
[8] S.H. Taylor, J.S.J. Hargreaves, G.J. Hutchings, R.W. Joyner, C.W. Lembacher, The partial oxidation of methane to methanol: An approach to catalyst design, Catal. Today 42 (1988) 217–224, https://doi.org/10.1016/S0920-5861(98)00095-9.
[9] N.D. Spencer, C.J. Pereira, V2O5-SiO2-catalyzed methane partial oxidation with molecular oxygen, J. Catal. 116 (1989) 399–406, https://doi.org/10.1016/0021-9517(89)90106-1.
[10] H. Bernd, A. Martin, A. Brückner, E. Schreier, D. Müller, H. Kosslick, G.-U. Wolf, B. Lücke, Structure and catalytic properties of VOx/MCM materials for the partial oxidation of methane to formaldehyde, J. Catal. 191 (2000) 384–400, https://doi.org/10.1006/jcat.1999.2786.
[11] T. Ito, J.H. Lunsford, Synthesis of ethylene and ethane by partial oxidation of methane over lithium-doped magnesium oxide, Nature 314 (1985) 721–722, https://doi.org/10.1038/314721b0.
[12] S.Y. Chen, D. Willcox, Effect of vanadium oxide loading on the selective oxidation of methane over V2Os/SiO2, Ind. Eng. Chem. Res. 32 (1993) 584–587, https://doi.org/10.1021/ie00016a002.
[13] A. Shilov, A.A. Shteinman, Activation of saturated hydrocarbons by metal complexes in solution, Coord. Chem. Rev. (1977) 97–143, https://doi.org/10.1016/S0010-8545(00)80336-7.
[14] R.A. Periana, D.J. Taube, E.R. Evitt, D.G. Loffler, P.R. Wentrcek, G. Voss, T. Masuda, A mercury-catalyzed, high-yield system for the oxidation of methane to methanol, Science 259 (1993) 340–343, https://doi.org/10.1126/science.259.5093.340.
[15] R.A. Periana, D.J. Taube, S. Gamble, H. Taube, T. Satoh, H. Fujii, Platinum catalysts for the high-yield oxidation of methane to a methanol derivative, Science 280 (1998) 560–564, https://doi.org/10.1126/science.280.5363.560.
[16] O.A. Mironov, S.M. Bischof, M.M. Konnick, B.G. Hashiguchi, V.R. Ziatdinov, W. A. Goddard, M. Ahlquist, R.A. Periana, Using reduced catalysts for oxidation reactions: mechanistic studies of the "Perianal-catalytica system" for CH4 oxidation, J. Am. Chem. Soc. 135 (2013) 14644–14658, https://doi.org/10.1021/ja404895z.

[17] N.V. Beznis, B.H. Weckhuysen, J.H. Bitter, Partial oxidation of methane over Co-ZSM-5: tuning the oxygenate selectivity by altering the preparation route, Catal. Lett. 136 (2010) 52–56, https://doi.org/10.1007/s10562-009-0206-6.
[18] J. Shen, W. Huang, L. Nguyen, Y. Yu, S. Zhang, Y. Li, A.I. Frenkel, F. Tao, Conversion of methane to methanol with a bent mono(μ-oxo)dinickel anchored on the internal surfaces of micropores, Langmuir 30 (2014) 8558–8569, https://doi.org/10.1021/la501184b.
[19] M.H. Mahyuddin, K. Yoshizawa, DFT exploration of active site motifs in methane hydroxylation by Ni-ZSM-5 zeolite, Catal. Sci. Technol. 8 (2018) 5875–5885, https://doi.org/10.1039/C8CY01441H.
[20] B.E.R. Snyder, P. Vanelderen, M.L. Bols, S.D. Hallaert, L.H. Böttger, L. Ungur, K. Pierloot, R.A. Schoonheydt, B.F. Sels, E.I. Solomon, The active site of low-temperature methane hydroxylation in iron-containing zeolites, Nature 536 (2016) 317–321, https://doi.org/10.1038/nature19059.
[21] E.M. Alayon, M. Nachtegaal, M. Ranocchiari, J.A. van Bokhoven, Catalytic conversion of methane to methanol over Cu-mordenite, Chem. Commun. 48 (2012) 404–406, https://doi.org/10.1039/C1CC15840F.
[22] D.K. Pappas, E. Borfecchia, M. Dyballa, I.A. Pankin, K.A. Lomachenko, A. Martini, M. Signorile, S. Teketel, B. Arstad, G. Berlier, C. Lamberti, S. Bordiga, U. Olsbye, K. P. Lillerud, S. Svelle, P. Beato, Methane to methanol: structure–activity relationships for Cu-CHA, J. Am. Chem. Soc. 139 (2017) 14961–14975, https://doi.org/10.1021/jacs.7b06472.
[23] M.J. Wulfers, S. Teletel, B. Ipek, R.F. Lobo, Conversion of methane to methanol on copper-containing small-pore zeolites and zeotypes, Chem. Commun. 51 (2015) 4447–4450, https://doi.org/10.1039/C4CC09645B.
[24] M.H. Mahyuddin, A. Staykov, Y. Shiota, M. Miyanishi, K. Yoshizawa, Roles of zeolite confinement and Cu-O-Cu angle on the direct conversion of methane to methanol by Cu2(μ-O)2+-exchanged AEI, CHA, AFX, and MFI zeolites, ACS Catal. 7 (2017) 3741–3751, https://doi.org/10.1021/acscatal.7b00588.
[25] S. Grundner, W. Luo, M. Sanchez-Sanchez, J.A. Lercher, Synthesis of single-site copper catalysts for methane partial oxidation, Chem. Commun. 52 (2016) 2553–2556, https://doi.org/10.1039/C5CC08371K.
[26] N.V. Beznis, B.M. Weckhuysen, J.H. Bitter, Cu-ZSM-5 zeolites for the formation of methanol from methane and oxygen: Probing the active sites and spectator species, Catal. Lett. 138 (2010) 14–22, https://doi.org/10.1007/s10562-010-0380-6.
[27] P. Tomkins, A. Mansouri, S.E. Bozbag, F. Krumeich, M.B. Park, E.M.C. Alayon, M. Ranocchiari, J.A. van Bokhoven, Isothermal cyclic conversion of methane into methanol over copper-exchanged zeolite at low temperature, Angew. Chem. Int. Ed. 55 (2016) 5467–5471, https://doi.org/10.1002/anie.201511065.
[28] T. Sheppard, C.D. Hamill, A. Goguet, D.W. Rooney, J.M. Thompson, A low temperature, isothermal gas-phase system for conversion of methane to methanol over Cu-ZSM-5, Chem. Commun. 50 (2014) 11053–11055, https://doi.org/10.1039/C4CC02832E.
[29] P. Tomkins, M. Ranocchiari, J.A. van Bokhoven, Direct conversion of methane to methanol under mild condisions over Cu-zeolites and beyond, Acc. Chem. Res. 50 (2017) 418–425, https://doi.org/10.1021/acs.accounts.6b00534.
[30] K. Narsimhan, K. Iyoki, K. Dinh, Y. Román-Leshkov, Catalytic oxidation of methane into methanol over copper-exchanged zeolites with oxygen at low temperature, ACS Cent. Sci. 2 (2016) 424–429, https://doi.org/10.1021/acscentsci.6b00139.
[31] K.T. Dinh, M.M. Sullivan, K. Narsimhan, P. Serena, R., J. Meyer, M. Dincă, Y. Román-Leshkov, Continuous partial oxidation of methane to methanol catalyzed by diffusion-paired copper dimers in copper-exchanged zeolties, J. Am. Chem. Soc. 141 (2019) 11641–11650, https://doi.org/10.1021/jacs.9b04906.
[32] T. Ikuno, J. Zheng, A. Vjunov, M. Sanchez-Sanchez, M.A. Ortuño, D.R. Pahls, J. L. Fulton, D.M. Camaioni, Z. Li, D. Ray, B.L. Mehdi, N.D. Browning, O.K. Farha, J. T. Hupp, C.J. Cramer, L. Gagliardi, J.A. Lercher, Methane oxidation to methanol catalyzed by Cu-Oxo clusters stabilized in NU-1000 metal–organic framework, J. Am. Chem. Soc. 139 (2017) 10294–10301, https://doi.org/10.1021/jacs.7b02936.
[33] J. Zheng, J. Ye, M.A. Ortuño, J.L. Fulton, O.Y. Gutiérrez, D.M. Camaioni, R. Kishan Motkuri, Z. Li, T.E. Webber, B.L. Mehdi, N.D. Browning, R.L. Penn, O.K. Farha, J. T. Hupp, D.G. Truhlar, C.J. Cramer, J.A. Lercher, Selective methane oxidation to methanol on Cu-Oxo dimers stabilized by zrconia nodes of an NU-1000 metal–organic framework, J. Am. Chem. Soc. 141 (2019) 9292–9304, https://doi.org/10.1021/jacs.9b02902.
[34] Q. Wang, D. Astruc, State of the art and prospects in metal-organic framework (MOF)-based and MOF-derived nanocatalysis, Chem. Rev. 120 (2020) 1438–1511, https://doi.org/10.1021/acs.chemrev.9b00223.
[35] J. Baek, B. Rungtaweevoranit, X. Pei, M. Park, S.C. Fakra, Y.-S. Liu, R. Matheu, S. A. Alshmimri, S. Alshehri, C.A. Trickett, G.A. Somorjai, O.M. Yaghi, Bioinspired metal-organic framework catalysts for selective methane oxidation to methanol, J. Am. Chem. Soc. 140 (2018) 18208–18216, https://doi.org/10.1021/jacs.8b11525.
[36] D.Y. Osadchii, A.I. Olivos-Suarez, Á. Szécsényi, G. Li, M.A. Nasalevich, I. A. Dugulan, P. Serra Crespo, E.J.M. Hensen, S.L. Veber, M.V. Fedin, G. Sankar, E. A. Pidko, J. Gascon, Isolated Fe sites in metal organic frameworks catalyze the direct conversion of methane to methanol, ACS Catal. 8 (2018) 5542–5548, https://doi.org/10.1021/acscatal.8b00505.
[37] M. Ravi, M. Ranocchiari, J.A. van Bokhoven, The direct catalytic oxidation of methane to methanol–A critical assessment, Angew. Chem. Int. Ed. 56 (2017) 16464–16483, https://doi.org/10.1002/anie.201702550.
[38] V.L. Sushkevich, D. Palagin, M. Ranocchiari, J.A. van Bokhoven, Selective anaerobic oxidation of methane enables direct synthesis of methanol, Science 356 (2017) 523–527, https://doi.org/10.1126/science.aam9035.
[39] P. Vanelderen, J. Vancauwenbergh, B.F. Sels, R.A. Schoonheydt, Coordination chemistry and reactivity of copper in zeolites, Coord. Chem. Rev. 257 (2013) 483–494, https://doi.org/10.1016/j.ccr.2012.07.008.
[40] E. Borfecchia, P. Beato, S. Svelle, U. Olsbye, C. Lamberti, S. Bordiga, Cu-CHA – a model system for applied selective redox catalysis, Chem. Soc. Rev. 47 (2018) 8097–8133, https://doi.org/10.1039/C8CS00373D.
[41] M.H. Mahyuddin, Y. Shiota, K. Yoshizawa, Methane selective oxidation to methanol by metal-exchanged zeolites: a review of active sites and their reactivity, Catal. Sci. Technol. 9 (2019) 1744–1768, https://doi.org/10.1039/C8CY02414F.
[42] A.I. Olivos-Suarez, À. Szécsényi, E.J.M. Hensen, J. Ruiz-Martinez, E.A. Pidko, J. Gascon, Strategies for the direct catalytic valorization of methane using heterogeneous catalysis: challenges and opportunities, ACS Catal. 6 (2016) 2965–2981, https://doi.org/10.1021/acscatal.6b00428.
[43] R.S. Liu, M. Iwamoto, J.H. Lunsford, Partial oxidation of methane by nitrous oxide over molybdenum oxide supported on silica, J. Chem. Soc. Chem. Commun. (1982) 78–79, https://doi.org/10.1039/C39820000078.
[44] H.F. Liuu, R.S. Liu, K.Y. Liew, R.E. Johnson, J.H. Lunsford, Partial oxidation of methane by nitrous oxide over molybdenum on silica, J. Am. Chem. Soc. 106 (1984) 4117–4121, https://doi.org/10.1039/C39820000078.
[45] J.J. Zhen, C.H. Khan, K.B. Lewis, G.A. Somorjai, Partial oxidation of methane with nitrous oxide over V2Os-SiO2 catalyst, J. Catal. 94 (1985) 501–507, https://doi.org/10.1016/0021-9517(85)90214-3.
[46] O. Memioglu, B. Ipek, A potential catalyst for continuous methane partial oxidation to methanol using N2O: Cu-SSZ-39, Chem. Commun. 57 (2021) 1364–1367, https://doi.org/10.1039/D0CC06534J.
[47] B. Ipek, R.F. Lobo, Catalytic conversion of methane to methanol on Cu-SSZ-13 using N2O as oxidant, Chem. Commun. 52 (2016) 13401–13404, https://doi.org/10.1039/C6CC07893A.
[48] C. Hammond, M.M. Forde, M.H.A. Rahim, A. Thetford, Q. He, R.L. Jenkins, N. Dimitratos, J.A. Lopez-Sanchez, N.F. Dummer, D.M. Murphy, A.F. Carley, S. H. Taylor, D.J. Willock, E.E. Stangland, J. Kang, H. Hagen, C.J. Kiely, G. J. Hutchings, Direct catalytic conversion of methane to methanol in an aqueous medium by using copper-promoted Fe-ZSM-5, Angew. Chem. Int. Ed. 51 (2012) 5129–5133, https://doi.org/10.1002/anie.201108706.
[49] C. Hammond, R.L. Jenkins, N. Dimitratos, J.A. Lopez-Sanchez, M.H. ab Rahim, M. M. Forde, A. Thetford, D.M. Murphy, H. Hagen, E.E. Stangland, J.M. Moulijn, S. H. Taylor, D.J. Willock, G.J. Hutchings, Catalytic and mechanistic insights of the low-temperature selective oxidation of methane over Cu-promoted Fe-ZSM-5, Chem. Eur. J. 18 (2012) 15735–15745, https://doi.org/10.1002/chem.201202802.
[50] C. Hammond, N. Dimitratos, J.A. Lopez-Sanchez, R.L. Jenkins, G. Whiting, S. A. Kondrat, M.H. ab Rahim, M.M. Forde, A. Thetford, H. Hagen, E.E. Stangland, J. M. Moulijn, S.H. Taylor, D.J. Willock, G.J. Hutchings, Aqueous-phase methane oxidation over Fe-MFI zeolites; promotion through isomorphous framework substitution, ACS Catal. 3 (2013) 1835–1844, https://doi.org/10.1021/cs400288b.
[51] P. Xiao, Y. Wang, T. Nishitoba, J.N. Kondo, T. Yokoi, Selective oxidation of methane to methanol with H2O2 over an Fe-MFI zeolite catalyst using sulfolane solvent, Chem. Commun. 55 (2019) 2896–2899, https://doi.org/10.1039/C8CC10026H.
[52] K.T. Dinh, M.M. Sullivan, P. Serna, R.J. Meyer, M. Dincă, Y. Román-Leshkov, Viewpoint on the partial oxidation of methane to methanol using Cu- and Fe-exchanged zeolites, ACS Catal. 8 (2018) 8306–8313, https://doi.org/10.1021/acscatal.8b01180.
[53] B.E.R. Snyder, M.L. Bols, R.A. Schoonheydt, B.F. Sels, E.I. Solomon, Iron and copper active sites in zeolites and their correlation to metalloenzymes, Chem. Rev. 118 (2018) 2718–2768, https://doi.org/10.1021/acs.chemrev.7b00344.
[54] R.S. Hanson, T.E. Hanson, Methanotrophic bacteria, Microbiol. Rev. 60 (1996) 439–471.
[55] M. Merkx, D.A. Kopp, M.H. Sazinsky, J.L. Blazyk, J. Muandller, S.J. Lippard, Dioxygen activation and methane hydroxylation by soluble methane monooxygenase: a tale of two irons and three proteins, Angew. Chem. Int. Ed. 40 (2001) 2782–2807, https://doi.org/10.1002/1521-3773(20010803)40:15<2782::AID-ANIE2782>3.0.CO;2-P.
[56] S. Friedle, E. Reisner, S.J. Lippard, Current challenges of modeling diiron enzyme active sites for dioxygen activation by biomimetic synthetic complexes, Chem. Soc. Rev. 39 (2010) 2768–2779, https://doi.org/10.1039/C003079C.
[57] M. Ravi, V.L. Sushkevich, A.J. Knorpp, M.A. Newton, D. Palagin, A.B. Pinar, M. Ranocchiari, J.A. van Bokhoven, Misconceptions and challenges in methane-to-methanol over transition-metal-exchanged zeolites, Nat. Catal. 2 (2019) 485–494, https://doi.org/10.1038/s41929-019-0273-z.
[58] M. Lin, A. Sen, Direct catalytic conversion of methane to acetic acid in an aqueous medium, Nature 368 (1994) 509–511, https://doi.org/10.1038/368613a0.
[59] M. Lin, A. Sen, A highly catalytic system for the direct oxidation of lower alkanes by dioxygen in aqueous medium. A formal heterogeneous analog of alkane monooxygenases, J. Am. Chem. Soc. 114 (1992) 7307–7308, https://doi.org/10.1021/ja00044a059.
[60] M. Lin, T. Hogan, A. Sen, A highly catalytic bimetallic system for the low-temperature selective oxidation of methane and lower alkanes with dioxygen as the oxidant, J. Am. Chem. Soc. 119 (1997) 6048–6053, https://doi.org/10.1021/ja964371k.
[61] A. Sen, Catalytic functionalization of carbon-hydrogen and carbon-carbon bonds in protic media, Acc. Chem. Res. 31 (1998) 550–557, https://doi.org/10.1021/ar970290x.
[62] X. Wang, G. Qi, J. Xu, B. Li, C. Wang, F. Deng, NMR-spectroscopic evidence of intermediate-dependent pathways for acetic acid formation from methane and

carbon monoxide over a ZnZSM-5 zeolite catalyst, Angew. Chem. Int. Ed. 51 (2012) 3850–3853, https://doi.org/10.1002/anie.201108634.
[63] K. Narsimhan, V.K. Michaelis, G. Mathies, W.R. Gunther, R.G. Griffin, Y. Román-Leshkov, Methane to acetic acid over Cu-exchanged zeolites: mechanistic insights from a site-specific carbonylation reaction, J. Am. Chem. Soc. 137 (2015) 1825–1832, https://doi.org/10.1021/ja5106927.
[64] Y. Jiang, M. Hunger, W. Wang, On the reactivity of surface methoxy species in acidic zeolite, J. Am. Chem. Soc. 128 (2006) 11679–11692, https://doi.org/10.1021/ja061018y.
[65] T. Blasco, M. Boronat, P. Concepción, A. Corma, D. Law, J.A. Vidal-Moya, Carbonylation of methanol on metal-acid zeolites: Evidence for a mechanism involving a multisite active center, Angew. Chem. Int. Ed. 46 (2007) 3938–3941, https://doi.org/10.1002/anie.200700029.
[66] P. Heung, A. Bhan. G. J. Sunley, D.J. Law, E. Iglesia, Site requirements and elementary steps in dimethyl ether carbonylation catalyzed by acidic zeolites, J. Catal. 245 (2007) 110–123, https://doi.org/10.1016/j.jcat.2006.09.020.
[67] J. Shan, M. Li, Lawrence F. Allard, S. Lee, M. Flytzani-Stephanopoulos, Mild oxidation of methane to methanol or acetic acid on supported isolated rhodium catalysts, Nature 551 (2017) 605–608, https://doi.org/10.1038/nature24640.
[68] Y. Tang, Y. Li, V. Fung, D. Jiang, W. Huang, S. Zhang, Y. Iwasawa, T. Sakata, L. Nguyen, X. Zhang, A.I. Frenkel, F. Tao, Single rhodium atoms anchored in micropores for efficient transformation of methane under mild conditions, Nat. Commun. 9 (2018) 1231–1242, https://doi.org/10.1038/s41467-018-03235-7.
[69] T. Moteki, N. Tominaga, M. Ogura, CO-assisted direct methane conversion into C1 and C2 oxygenates over ZSM-5 supported transition and platinum group metal catalysts using oxygen as an oxidant, ChemCatChem 12 (2020) 2957–2961, https://doi.org/10.1002/cctc.202000168.
[70] S. Sogukkanli, T. Moteki, M. Ogura, Masaru, selective methanol formation via CO-assisted direct partial oxidation of methane over copper containing CHA-type zeolites prepared by one-pot synthesis, Green. Chem. 23 (2021) 2148–2154, https://doi.org/10.1039/D0GC03645E.
[71] R.H. Bunting, J. Thompson, P. Hu, The mechanism and ligand effects of single atom rhodium supported on ZSM-5 for the selective oxidation of methane to methanol, Phys. Chem. Chem. Phys. 22 (2020) 11686–11694, https://doi.org/10.1039/D0CP01284J.
[72] J. Qi, P. Christopher, Atomically dispersed Rh active sites on oxide supports with controlled acidity for gas-phase halide-free methanol carbonylation to acetic acid, Ind. Eng. Chem. Res. 58 (2019) 12632–12641, https://doi.org/10.1021/acs.iecr.9b02289.
[73] Q. Sun, N. Wang, T. Zhang, R. Bai, A. Mayoral, P. Zhang, Q. Zhang, O. Terasaki, J. Yu, Zeolite-exchanged single atom rhodium catalysts: highly-efficient hydrogen generation and shape-selective tandem hydrogenation of nitroarenes, Angew. Chem. Int. Ed. 58 (2019) 18570–18576, https://doi.org/10.1002/anie.201912367.
[74] Y. Liu, Z. Li, Q. Yu, Y. Chen, Z. Chai, G. Zhao, S. Liu, Q.-C. Cheong, Y. Pan, Q. Zhang, L. Gu, L. Zheng, Y. Wang, Y. Lu, D. Wang, C. Chen, Q. Peng, Y. Liu, L. Liu, J. Chen, Y. Li, A general strategy for fabricating isolated single metal atomic site catalysts in Y zeolite, J. Am. Chem. Soc. 141 (2019) 9305–9311, https://doi.org/10.1021/jacs.9b02936.
[75] J.D. Kistler, N. Chotigkrai, P. Xu, B. Enderle, P. Praserthdam, C.-Y. Chen, N. D. Browning, B.C. Gates, A single-site platinum CO oxidation catalyst in zeolite KLTL: microscopic and spectroscopic determination of the locations of the platinum atoms, Angew. Chem. Int. Ed. 53 (2014) 8904–8907, https://doi.org/10.1002/anie.201403353.
[76] M. Moliner, J.E. Gabay, C. Kliewer E., R.T. Carr, J. Guzman, G, L. Casty, P. Serna, A. Corma, Reversible transformation of Pt nanoparticles into single atoms inside high-silica chabazite zeolite, J. Am. Chem. Soc. 138 (2016) 15743–15750, https://doi.org/10.1021/jacs.6b10169.
[77] B.C. Gates, M. Flytzani-Stephanopoulos, D.A. Dixon, A. Katz, Atomically dispersed supported metal catalysts: perspectives and suggestions for future research, Catal. Sci. Technol. 7 (2017) 4259–4275, https://doi.org/10.1039/C7CY00881C.
[78] H. Matsubara, K. Yamamoto, E. Tsuji, K. Okumura. K. Nakamura, S. Suganuma, N. Katada, Position and Lewis acidic property of active cobalt species on MFI zeolite for catalytic methylation of benzene with methane, Microporous Mesoporous Mater. 310 (2021), 110649, https://doi.org/10.1016/j.micromeso.2020.110649.
[79] H. Matsubara, E. Tsuji, Y. Moriwaki, K. Okumura, K. Yamamoto, K. Nakamura, S. Suganuma, N. Katada, Selective formation of active cobalt species for direct methylation of benzene with methane on MFI Zeolite by co-presence of secondary elements, Catal. Lett. 149 (2019) 2627–2635, https://doi.org/10.1007/s10562-019-02855-y.
[80] R.A. Periana, O. Mironov, D. Taube, G. Bhalla, C.J. Jones, Catalytic, oxidative condensation of CH4 to CH3COOH in one step via CH activation, Science 301 (2003) 814–818, https://doi.org/10.1126/science.1086466.
[81] X. Wang, G. Qi, J. Xu, B. Li, C. Wang, F. Deng, NMR-spectroscopic evidence of intermediate-dependent pathways for acetic acid formation from methane and carbon monoxide over a ZnZSM-5 zeolite catalyst, Angew. Chem. Int. Ed. 51 (2012) 3850–3853, https://doi.org/10.1002/anie.201108634.
[82] K.J. Cavell, Recent fundamental studies on migratory insertion into metal-carbon bonds, Coord. Chem. Rev. 155 (1996) 209–243, https://doi.org/10.1016/S0010-8545(96)90182-4.
[83] T. Moteki, N. Tominaga, N. Tsunoji, T. Yokoi, M. Ogura, Impact of the zeolite cage structure on product selectivity in CO-assisted direct partial oxidation of methane over Rh supported AEI-, CHA-, and AFX-type zeolites, Chem. Lett. 50 (2021) 1597–1600, https://doi.org/ 1 0.1246/cl.210250.
[84] Database of Zeolite Structure. ⟨http://www.iza-structure.org/databases/⟩, 2003 (accessed 20 May 2021).
[85] J. Jae, G.A. Tompsett, A.J. Foster, K.D. Hammond, S.M. Auerbach, R.F. Lobo, G. W. Huber, Investigation into the shape selectivity of zeolite catalysts for biomass conversion, J. Catal. 279 (2011) 257–268, https://doi.org/10.1016/j.jcat.2011.01.019.
[86] M.E. van Leeuwen, Derivation of stockmayer potential parameters for polar fluids, Fluid Phase Equilib. 99 (1994) 1–18, https://doi.org/10.1016/0378-3812(94)80018-9.